Experimental and theoretical study of the infrared spectra of $BrHI^-$ and $BrDI^-$

M. J. Nee, A. Osterwalder, and D. M. Neumark[a)]
Department of Chemistry, University of California, Berkeley, California 94720 and Chemical Sciences Division, Lawrence Berkeley Laboratory, Berkeley, California 94720

C. Kaposta and C. Cibrián Uhalte
Institut für Experimentalphysik, Freie Universität Berlin, Arnimallee 14, 14195 Berlin, Germany

T. Xie, A. Kaledin, and J. M. Bowman[b)]
Department of Chemistry and Cherry L. Emerson Center for Scientific Computation, Emory University, Atlanta, Georgia 30322

S. Carter
Department of Chemistry, University of Reading, Reading, United Kingdom

K. R. Asmis[c)]
Fritz-Haber-Institut der Max-Planck-Gesellschaft, Faradayweg 4-6, 14195 Berlin, Germany

(Received 19 July 2004; accepted 27 July 2004)

Gas phase vibrational spectra of $BrHI^-$ and $BrDI^-$ have been measured from 6 to 17 μm (590–1666 cm^{-1}) using tunable infrared radiation from the free electron laser for infrared experiments in order to characterize the strong hydrogen bond in these species. $BrHI^- \cdot Ar$ and $BrDI^- \cdot Ar$ complexes were produced and mass selected, and the depletion of their signal due to vibrational predissociation was monitored as a function of photon energy. Additionally, $BrHI^-$ and $BrDI^-$ were dissociated into HBr (DBr) and I^- via resonant infrared multiphoton dissociation. The spectra show numerous transitions, which had not been observed by previous matrix studies. New *ab initio* calculations of the potential-energy surface and the dipole moment are presented and are used in variational ro-vibrational calculations to assign the spectral features. These calculations highlight the importance of basis set in the simulation of heavy atoms such as iodine. Further, they demonstrate extensive mode mixing between the bend and the H-atom stretch modes in $BrHI^-$ and $BrDI^-$ due to Fermi resonances. These interactions result in major deviations from simple harmonic estimates of the vibrational energies. As a result of this new analysis, previous matrix-isolation spectra assignments are reevaluated. © *2004 American Institute of Physics.*
[DOI: 10.1063/1.1794671]

I. INTRODUCTION

The triatomic hydrogen bihalide anions, XHY^-, where X and Y are halogen atoms, are of fundamental chemical interest. From the perspective of electronic structure, these anions are an important model system for understanding three-center bonding.[1,2] They have some of the strongest hydrogen bonds known, as evidenced by their high dissociation energies relative to $X^- + HY$ (1.7 eV for FHF^-)[3] and low-frequency hydrogen stretch vibrations (723 cm^{-1} for $BrHBr^-$).[4] Bihalide anions also serve as transition state precursors in negative ion photoelectron (PE) spectroscopy experiments, in which it has been shown that photodetachment of the anion can access the transition state region of the X+HY reaction.[5,6] Interpretation of these experiments is strongly dependent on the quality of the spectroscopic and structural data available for the anion. Infrared (IR) spectra of several symmetric XHX^- anions have been measured via matrix-isolation spectroscopy[7] and in the gas phase,[4,8,9] and are reasonably well understood. The matrix IR spectra of the asymmetric ($X \neq Y$) bihalides[10] are more complex, however, and have so far only been interpreted by assuming the simultaneous presence of two structural forms of the anions. Clearly, gas phase IR spectra are desirable to gain an improved understanding of these species. Here, we report the first such spectrum of an asymmetric bihalide, $BrHI^-$, using a tunable infrared free electron laser (FEL) to perform vibrational predissociation spectroscopy on $BrHI^- \cdot Ar$ and resonant infrared multiphoton dissociation (IRMPD) experiments on bare $BrHI^-$. Identical experiments are described for the deuterated analogs.

The $BrHI^-$ anion was first observed by Ellison and Ault[10] using IR matrix-isolation spectroscopy. They observed four bands at 666, 799, 920, and 1171 cm^{-1} for $BrHI^-$ and three bands at 470, 728, and 862 cm^{-1} for $BrDI^-$. Previous work on symmetric bihalides[11] in matrices showed that, depending on conditions, one could generate symmetric (type II) and asymmetric (type I) forms of the anion, with type II anions exhibiting considerably lower H-atom stretch (υ_3) frequencies owing to a greater delocalization of the hydro-

a)Electronic mail: dan@radon.cchem.berkeley.edu
b)Electronic mail: bowman@euch4e.chem.emory.edu
c)Electronic mail: asmis@physik.fu-berlin.de

gen. Ellison and Ault[10] assigned the $BrHI^-$ spectrum assuming that this ion also existed in two forms, both with asymmetric hydrogen bonds, but with a more localized and asymmetric hydrogen bond in the type I structure than the type II structure. The $BrHI^-$ peaks at 920 and 1171 cm^{-1} were assigned to the type I ion; the peak at 920 cm^{-1} was assigned to the υ_3 fundamental and that at 1171 cm^{-1} to either the fundamental or overtone of the υ_2 bending mode. The other two peaks at 666 and 799 cm^{-1} were assigned to the type II structure, in which the hydrogen is shared more equally between the bromine and iodine. Unlike their symmetric counterparts, all of the $BrHI^-$ matrix peaks were seen regardless of the preparation conditions. For the XHX^- anions, the type I structures were attributed to strong perturbation by the matrix, implying that the gas phase geometry would be closer to the type II structure. This expectation has been borne out in the gas phase IR spectra of FHF^-, $ClHCl^-$, and $BrHBr^-$,[4,8,9] in which the υ_3 antisymmetric stretch frequencies seen are very close to the type II matrix values. However, the question of which structure, if either, exists in the gas phase has remained open for the asymmetric bihalides.

In the gas phase, Caldwell and Kebarle[3] measured the dissociation energy of $BrHI^-$ relative to the $I^- + HBr$ limit at 0.70 eV. The gas phase PE spectra of $BrHI^-$ and $BrHI^- \cdot Ar$ have been reported and analyzed in a series of papers by Neumark and co-workers.[12–14] These spectra showed resolved vibrational structure that was close to but noticeably lower in frequency than the diatomic HBr vibrational frequency, indicating that photodetachment of the anion accessed the I+HBr product valley of the neutral Br+HI potential energy surface (PES) rather than the $[BrHI]^‡$ transition state. This interpretation is consistent with the expected asymmetric $I^- \cdots HBr$ structure of the anion, reflecting the higher proton affinity of Br^- relative to I^- (by 0.40 eV).[15] Wave packet simulations by Bradforth *et al.*,[12] using a highly simplified potential function for the anion and a model potential energy surface[16] for the Br+HI reaction, produced reasonable agreement with the experimental spectra. In these simulations, the anion υ_3 frequency was assumed to be 920 cm^{-1} based on the type I value from the matrix studies; a satisfactory simulation of the PE spectra could not be obtained using the type II value (666 cm^{-1}). However, given the approximations made by Bradforth *et al.*, this result alone does not constitute definitive support for the type I anion in the gas phase.

In order to gain a more complete understanding of the photoelectron spectrum of $BrHI^-$, Kaledin *et al.*[17] constructed an *ab initio* potential energy surface for the anion and performed variational ro-vibrational calculations to determine the energy eigenvalues. These calculations recovered the experimental dissociation energy of the complex and confirmed the linear, asymmetric geometry. The calculations found the H–Br equilibrium bond distance, r_{HBr}, to be substantially shorter than the H–I distance, r_{HI} (1.50 versus 2.31 Å) and only slightly longer than the equilibrium bond length in diatomic H–Br (1.414 Å).[18] The full-dimensionality calculation of the vibrational energy levels yielded 1266.7 cm^{-1} for the υ_3 fundamental, considerably lower than the *ab initio* harmonic value, 1779 cm^{-1}, but more than 300 cm^{-1} above the type I matrix value, 920 cm^{-1} (and even further above the type II value). If these calculations are correct, they indicate that either the matrix experiment was misassigned or that the matrix shift was abnormally large.

Measurement of the gas phase infrared spectra of these ions should resolve the discrepancies between the matrix spectra and the calculations. However, the frequency range of interest is too low for the tunable IR lasers typically used in the vibrational spectroscopy of ions. Meijer and co-workers[19–21] have measured low-frequency vibrations in clusters and other species with vibrational action spectroscopy using a tunable infrared free-electron laser. Asmis and co-workers[8,22,23] used this light source to obtain vibrational spectra of strongly hydrogen-bonded cationic and anionic complexes from 600 to 1500 cm^{-1}, where vibrational frequencies associated with the shared hydrogen are expected. As in the experiments by Okumura *et al.*,[24] Bieske *et al.*,[25] and Ayotte *et al.*,[26] a weakly bound ''messenger'' atom may be added to the species being investigated, which leaves the vibrationally excited ion via vibrational predissociation (VPD). Alternatively, resonant IRMPD may be used to dissociate the unclustered chromophore. In either case, detection is accomplished by monitoring parent ion depletion or fragment ion formation as a function of photon energy. In this work, we obtain gas phase vibrational spectra of $BrHI^-$ and $BrDI^-$ using VPD on $BrHI^- \cdot Ar$ and $BrDI^- \cdot Ar$ and IRMPD on the bare anions in order to gain further insight into hydrogen bonding in the asymmetric hydrogen bihalides and to aid in the construction of an improved anion potential energy surface.

The spectra presented here are then compared with the new calculations on $BrHI^-$ and $BrDI^-$. These calculations are similar to those presented previously by Kaledin *et al.*[17] but use a better method and a larger electronic basis to calculate the anion potential energy surface; a calculation of the dipole moment surface is also done for the first time. The new potential energy and dipole surfaces are used to simulate ro-vibrational energies and transition intensities. The new calculations reproduce the experimental transition energies and intensities and are in significantly better agreement with the experiment than the earlier calculations of Kaledin *et al.*[17] They show considerable mode mixing between the H-atom stretch and bending modes, thus explaining the complexity of the new infrared spectra. The spectra and calculations provide the most complete picture currently available for an asymmetric bihalide anion.

II. EXPERIMENT

All experiments were performed on a tandem mass spectrometer ion trap system at the free electron laser for infrared experiments (FELIX) facility [Stichting voor Fundamenteel Onderzoek der Materie (FOM)-Institute for Plasma Physics ''Rijnhuizen,'' Nieuwegein, The Netherlands]. The apparatus, including its use in conjunction with the FELIX, has been discussed previously[27] and is described only briefly here. All ions are generated by crossing a pulsed (100 Hz) supersonic expansion of the appropriate gas mix with a beam of electrons from a 300-μA, 1-keV electron gun. The gas

TABLE I. Comparison of the optimized geometries (angstroms or deg) and normal-mode frequencies (cm^{-1}) with different basis sets. All calculations were done by the coupled cluster method [CCSD(T)] if not specified otherwise. For the vibrational frequencies, ω_1, ω_2, and ω_3 correspond to the halogen stretch, bend, and H-atom stretch modes, respectively.

Basis sets	r_{HBr}	r_{HI}	θ_{BrHI}	ω_1	ω_2	ω_3
Previous study[a]	1.499	2.318	180	85	550	1726
AVTZ	1.530	2.186	180	110	600	1481
AVTZ (cpp)[b]	1.527	2.171	180	112	604	1476
AVQZ[c]	1.524	2.196	180	105	587	1500
AVQZ[c] (cpp)	1.521	2.180	180	107	592	1487
AVQZ	1.525	2.203	180	106	574	1513
AVQZ (cpp)	1.523	2.185	180	108	581	1500
AVQZ[c] (cpp)/MRCI	1.512	2.206	180	108	591	1570
Fitted surface by MRCI	1.512	2.207	180	100	613	1543

[a]From Ref. 17: Stuttgart quasirelativistic ECP with valence $3s3p1d$ contraction with a diffuse s augmentation for the halogens and 6-311G(p) for the hydrogen.
[b]Core polarization potential.
[c]No g functions included in the basis set.

mix used was between 0.05% and 0.5% HBr (or DBr) in argon (higher HBr concentrations for bare $BrHI^-$ clusters, lower for $BrHI^- \cdot Ar$), passed over a small quantity of methyl iodide, then expanded into the vacuum via a pulsed molecular beam valve (General Valve). The ions produced from the expansion pass through a 2-mm-diameter skimmer. The negative ion beam is collimated by a gas-filled radio frequency (rf) decapole ion guide and then directed into a quadrupole mass filter. The mass-selected anions are collected in a linear rf hexadecapole ion trap, which is filled with a background pressure of approximately 0.015 mbar of helium and connected to the head of a closed cycle helium cryostat held at 16 K. For typical IRMPD experiments, the trap is filled for 150 ms (500 ms for the VPD experiments), corresponding to approximately 15 gas pulses being stored before interacting with the field. Because FELIX runs at 5 Hz, it is preferable to store for less than 200 ms to take full advantage of each FELIX pulse. However, for the $BrHI^- \cdot Ar$ and $BrDI^- \cdot Ar$ experiments, longer storage times were needed to compensate for the lower numbers produced and for the loss in the trap.

The FELIX radiation used for these experiments ranges from 6 to 17 μm (1666–590 cm^{-1}) with a bandwidth on the order of 0.4% of the central energy (full width at half maximum); it enters the trap collinearly with the ions. Typical powers are the order of 300 mW at the center of the range but decrease significantly at the lower wavelengths in the range used (less than 7 μm) to about 100 mW. Additionally, each 5-μs macropulse contains a series of several thousand micropulses, each approximately 1 ps in duration, with about 1 ns between micropulses. To increase the photon density in the trap, the beam is focused at the center of the interaction region using a 50-cm focal length KBr lens. The calibration of FELIX is achieved by an external spectral analyzer.

Approximately 1 ms after their interaction with the radiation field, the ions are emptied from the trap and directed into a second quadrupole mass filter, which separates the fragment ions from their undissociated parent ions for detection. For the weakly bound $BrHI^- \cdot Ar$ and $BrDI^- \cdot Ar$ complexes, collisional cooling with the helium in the ion trap causes significant dissociation. Approximately 80% of the complexes dissociate due to collisions in this case, but because this number is constant over the course of a stably running experiment, the parent complex depletion is monitored to produce a predissociation spectrum. In the $BrHI^-$ and $BrDI^-$ multiphoton experiments, monitoring the I^- daughter fragment produces more satisfactory results because of a near-zero background. Although parent ion depletion was sometimes visible, it was generally much smaller than in the VPD experiments and was difficult to detect on such a large background. Br^- appearance could also sometimes be observed but yielded no additional peaks.

III. THEORETICAL METHODS

A. Potential-energy surface and dipole moment

The electronic energy calculations and fitting are similar to the procedures used previously by Kaledin *et al.*[17] In those calculations of the anion surface, the coupled cluster method was used and several high-energy configurations posed convergence problems. Moreover, bond breaking and the breakup limit, i.e., $I^- \cdots H \cdots Br$, cannot be properly described with a single reference method. In this work, we use the more versatile multireference configuration interaction (MRCI) approach to map the surface with a future aim of investigating excited electronic states and spin-orbit coupling. We correct for non-size extensivity of MRCI by including Davidson's correction. Also, several basis sets, larger than those used previously, were investigated. For the effective core potential (ECP) for Br and I, the Stuttgart ECP set, which includes both f [for (AVTZ) basis] and g [for (AVQZ) basis] functions for Br and I, was used.[28] In our MRCI calculations, we use 31 reference configurations out of full valence complete active space with 16 electrons distributed in nine molecular orbitals. The final contracted configuration interaction contains around half a million configurations for the AVQZ basis without g functions. These calculations were performed with the MOLPRO quantum chemistry package.[29]

In Table I, we compare the geometries and harmonic frequencies calculated with different basis sets. In order to

make a comparison with our previous work,[17] we have used the coupled cluster singles and doubles with perturbative triples [CCSD(T)] method (which was used previously) in these calculations. We also include the results from the present MRCI calculations using the basis that was used to obtain the potential surface and the results from the potential surface. Comparison of the optimized geometries from the old and new basis sets shows that the biggest difference lies in r_{HI}, which is compressed by 0.13 Å using the new basis. In contrast, r_{HBr} increases by only about 0.02 Å. The harmonic frequencies at the equilibrium structure are also shifted significantly. The halogen stretch is blueshifted by about 20 cm^{-1}, a relative change of 23%; the H-atom stretch is redshifted by about 220 cm^{-1}, a relative change of 13%. This comparison clearly shows the importance of the *f* function for the halogen atoms and the necessity of constructing a PES using a large basis set. To determine the optimal basis set for the new PES, the convergence of the properties shown in Table I was monitored. As seen, the inclusion of *g* functions does not have a significant effect on the optimized geometries or the vibrational frequencies. On the other hand, the core-polarization potential (cpp)[30] term seems to give an appreciable correction with very little additional cost. Thus, the AVQZ basis (without *g* functions) with the Stuttgart ECP, including the core-polarization effect, was used as the basis for the electronic energy and dipole moment calculations. The CCSD(T) and MRCI optimized geometry and harmonic frequencies are in good agreement with each other (for the same basis), as expected. Also, the fitted potential reproduces the *ab initio* MRCI values well.

The IR intensities were calculated using MOLPRO in the standard double-harmonic approximation, yielding 0.00, (0.04 0.04), and 4908 km/mol for the halogen stretch, the (doubly degenerate) bend, and the H-atom stretch, respectively. Thus, these approximate calculations predict virtually no IR intensity for the halogen stretch and bend modes.

For the construction of the PES, 2268 *ab initio* energy points were computed on a regular three-dimensional (3D) grid defined by r_{HBr}[1.0,1.15,1.28,1.38,1.46,r_e=1.513, 1.57, 1.65, 1.75,2.0,2.4,3.0,4.0,5.0] Å, r_{HI} [1.35,1.62,1.82, 1.94, 2.02,2.09,2.15, r_e = 2.205, 2.25, 2.32, 2.41, 2.53, 2.7,3.0, 3.7,5.0,7.0,9.0] Å, and θ_{BrHI}[180,177,172,165,155,140,120, 100,80] deg. It should be noted that there is another stationary collinear structure of the anion with Br in the middle, which is not covered in this grid. As has been discussed in the previous paper,[17] the energy for this second minimum is too high to contribute to the low-lying vibrational states. The electronic energies and dipole moment were fit by a 3D spline, which was used in the ro-vibrational calculations described next.

B. Ro-vibrational calculations

The ro-vibrational bound-state variational calculations were carried out using two very different codes. One uses a Hamiltonian in Jacobi coordinates and a truncation/recoupling procedure as described in detail previously.[17] The other code, RVIB3,[31–33] uses a Hamiltonian in terms of two bond lengths, r_{HBr} and r_{HI}, and the bond angle θ_{BrHI}. Infrared transition probabilities were obtained from both codes by integrating dipole moment matrix elements over both the vibrational and rotational coordinates (the details of the "exact" calculations done in RVIB3 can be found in Ref. 32). These intensity calculations assumed $J=0$ to be the initial state of the anion and were done for final $J=1$ and $|\Delta K| = 0$ or 1, in accord with standard dipole selection rules. Parallel transitions, i.e., $\Delta K=0$, couple the initial state to excited bending states with an even quanta of bend excitation.

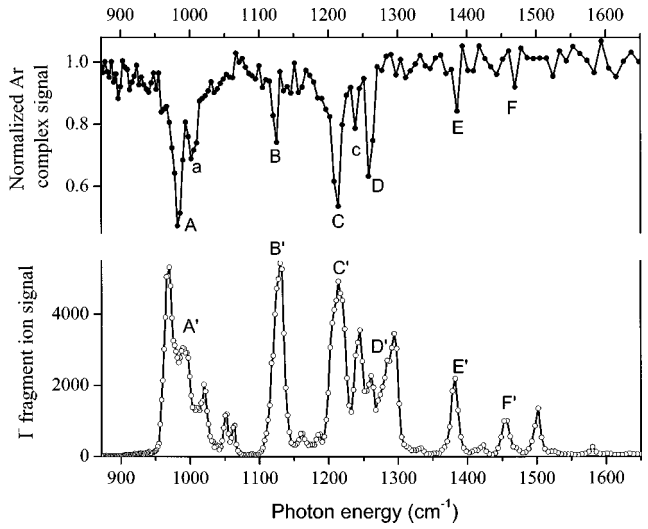

FIG. 1. Infrared dissociation spectra of $\mathrm{BrHI}^- \cdot \mathrm{Ar}$ (closed circles, upper trace) and BrHI^- (open circles, lower trace). Peaks in the $\mathrm{BrHI}^- \cdot \mathrm{Ar}$ predissociation spectrum, where the parent ion depletion is monitored, point downward, whereas the multiphoton spectrum of BrHI^- has upward peaks because the I^- fragment ion is monitored.

IV. RESULTS

A. Predissociation spectra

Parent ion depletion spectra for $\mathrm{BrHI}^- \cdot \mathrm{Ar}$ and $\mathrm{BrDI}^- \cdot \mathrm{Ar}$ are shown in the top traces of Figs. 1 and 2, respectively. Both spectra are scaled to the field-free background. The corresponding peak positions are given in Tables II and III.

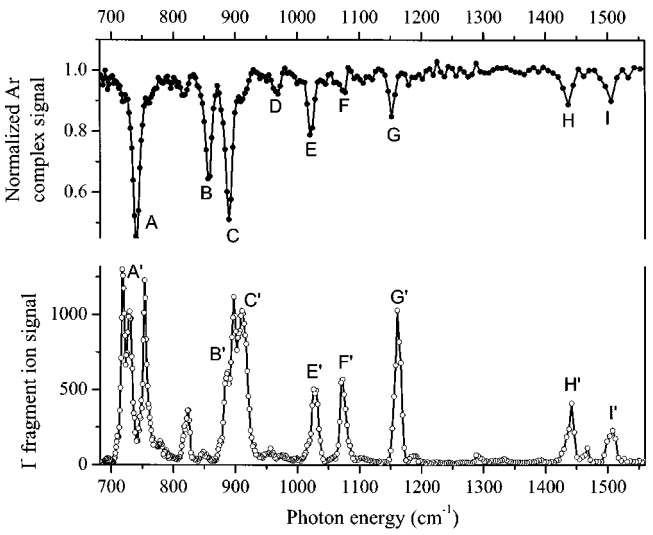

FIG. 2. Infrared dissociation spectra of $\mathrm{BrDI}^- \cdot \mathrm{Ar}$ (closed circles, upper trace) and BrDI^- (open circles, lower trace).

TABLE II. Peak assignments for predissociation spectra of $BrHI^- \cdot Ar$. Experimental intensities in brackets have been corrected and rescaled to the largest value to account for the number of photons.

Peak label	Peak position (cm^{-1})		Assignment ($n_1\ n_2\ n_3$)	Intensity	
	Experiment	Calculation		Experiment [Corrected]	Calculation
A	984	983.2	0 2 0+0 0 1	1.0 [0.75]	1.0
a	1003	⋯	$(0\ 2\ 0+0\ 0\ 1)+v_{Ar}$	0.58 [0.39]	⋯
B	1127	1126.9	1 2 0+1 0 1	0.49 [0.40]	0.014
C	1215	1228.0	0 2 0−0 0 1	0.86 [1.00]	0.23
c	1238	⋯	$(0\ 2\ 0-0\ 0\ 1)+v_{Ar}$	0.39 [0.40]	⋯
D	1259	1268.1	2 2 0+2 0 1	0.70 [0.80]	0.12
E	1380	1390.0	3 2 0+3 0 1	0.30 [0.40]	0.0029
F	1468	1462.4	2 2 0−2 0 1	0.14 [0.25]	0.00050

The spectra in each case were taken at steps of 0.01 μm. Peaks *A* and *C* at 984 and 1215 cm^{-1} for $BrHI^- \cdot Ar$ and 742 and 890 cm^{-1} for $BrDI^- \cdot Ar$ are the most intense features in each spectrum. In each case, they correspond closely to the two higher energy peaks seen in Ellison and Ault's matrix work (920 and 1171 cm^{-1} in $BrHI^-$, 730 and 861 cm^{-1} for $BrDI^-$).[10] All four matrix values are lower than the corresponding gas phase frequencies, with redshifts varying from 12 cm^{-1} (peak *A*, $BrDI^-$) to 64 cm^{-1} (peak *A*, $BrHI^-$). As discussed in Sec. I, the higher-energy matrix peaks were attributed to the more asymmetric type I anion structure. No peaks assigned to the type II structure are observed in the gas phase, although the peaks should be well within the range of the FELIX radiation used, implying that only the type I structure is observed in the gas phase. However, as will be discussed below, the peaks presented cannot be assigned as simply as was done in the matrix work.

In addition, several peaks that were not seen previously are present in both spectra. Peaks *A*, *B*, and *D* in $BrHI^- \cdot Ar$ are approximately evenly spaced (143 cm^{-1} between *A* and *B*, 132 cm^{-1} between *B* and *D*). In $BrDI^- \cdot Ar$, peaks *A*, *B*, *D*, and *F* are spaced by approximately 110 cm^{-1} and *C*, *E*, and *G* by about 130 cm^{-1}. This pattern suggests combination bands involving the low-frequency v_1 stretch, primarily a heavy-atom vibration in these anions. A more definitive assignment emerges from comparison with the simulations in Sec. V. Also present is a small peak (labeled peak *a*) to the blue of peak *A* in $BrHI^- \cdot Ar$, which does not appear as

TABLE III. Peak Assignments for predissociation spectra of $BrDI^- \cdot Ar$. Experimental intensities in brackets have been corrected and rescaled to the largest value to account for the number of photons.

Peak label	Peak position (cm^{-1})		Assignment ($n_1\ n_2\ n_3$)	Intensity	
	Experiment	Calculation		Experiment [Corrected]	Calculation
A	742	747.9	020+001	1.0 [0.95]	1.0
B	857	864.2	120+101	0.65 [0.64]	0.15
C	890	910.5	020−001	0.89 [1.00]	0.53
D	970	971.7	220+201	0.15 [0.14]	0.00070
E	1021	1041.9	120−101	0.38 [0.45]	0.025
F	1080	1077.3	320+301	0.13 [0.17]	0.0084
G	1154	1165.4	220−201	0.27 [0.38]	0.0074
H	1433	1448.2	040+002	0.20 [0.57]	0.095
I	1502	1520.9	040−002	0.18 [0.66]	0.026

TABLE IV. Peak assignments for multiphoton dissociation of $BrHI^-$. Values in brackets are divided by two to show the expected two-photon frequency.

Peak label	Peak position (cm^{-1}) Experiment	Calculation [÷2]	Assignment	Number of photons
A'	971	1939.3 [969.7]	040+002	2
	988	983.2	020+001	1
	1018	2035.6 [1017.8]	040−002	2
	1051	2107.9 [1054.0]	140+102	2
	1064	2123.4 [1061.7]	140−102	2
B'	1127	1126.9	120+101	1
	1162	2332.2 [1166.1]	240−202	2
	1187	2375.6 [1187.8]	340+302	2
C'	1213	1228.0	020−001	1
	1244	2445.2 [1222.6]	340−302	2
		2457.7 [1228.9]	021	2
D'	1262	1268.1	220+201	1
	1294	2599.6 [1299.8]	121	2
	1333	1339.0	120−101	1
E'	1382	1390.0	320+301	1
	1423	2857 [1428.5]	221	2
F	1455	1462.4	220−201	1
	1498	1498.9	420+401	1
	1580	1587.1	520+501	1

TABLE V. Peak assignments for multiphoton dissociation of $BrDI^-$. Values in brackets are divided by two to show the expected two-photon frequency.

Peak label	Peak position (cm^{-1}) Experiment	Calculation [÷2]	Assignment	Number of photons
A'	719	1448.2 [724.1]	040+002	2
	730	747.9	020+001	1
	755	1520.9 [760.5]	040−002	2
	779	1582.9 [791.5]	140+102	2
	827	1645.3 [822.7]	140−102	2
	848	1691.1 [845.6]	240+202	2
B'	886	864.2	120+101	1
	900	1801.1 [900.6]	240−202	2
C'	911	910.5	020−001	1
		1819.9 [910.0]	021	2
	956	1939.4 [969.7]	121	2
		971.7	220+201	1
E'	1029	1041.9	120−101	1
F'	1073	1077.3	320+301	1
G'	1164	1165.4	220−201	1
	1188	1185.7	320−301	1
	1291	1305.5	420+401	1
H'	1442	1448.2	040+002	1
	1466	1429.3	420−401	1
I'	1509	1520.9	040−002	1

prominently in the $BrDI^- \cdot Ar$ spectrum. Similarly, a small peak (peak *c*) is seen to the blue of peak *C* in $BrHI^- \cdot Ar$. Both of these small peaks are approximately 20 cm^{-1} separated from the preceding peak.

Finally, Tables II and III present the experimental depletion intensities for comparison with the theoretical transition strengths. The experimental values are actually given by $-\ln(c/c_0)$, where c/c_0 is the depletion signal read from Figs. 1 and 2. Here, we assume that all the complexes vibrationally excited by each micropulse dissociate before the next micropulse 1 ns later, so that there is a steadily decreasing number of ions interacting with the successive micropulses. Under these circumstances, it is $-\ln(c/c_0)$ that is proportional to the transition strength. Additionally, the intensities scaled to the photon flux at each wavelength are listed in square brackets in order to account for the decreased flux at the higher-frequency range of the spectra in Figs. 1 and 2. Both sets of values have been normalized to set the most intense peak to unity.

B. Multiphoton spectra

The dissociation spectra of bare $BrHI^-$ and $BrDI^-$ obtained by monitoring I^- fragment production are shown in the lower traces of Figs. 1 and 2, respectively. Line positions are given in Tables IV and V. There are clear correspondences between the vibrational predissociation and multiphoton spectra, as is emphasized by the labeling scheme (*A* versus A', etc.) used in the two sets of spectra. There are, however, significant differences. There are more peaks in the multiphoton spectra and many of the smaller peaks are more intense than in the VPD spectra. The main peaks (*A* and *C*) in the VPD spectra appear as clusters of closely spaced peaks in the IRMPD spectra. Finally, there is usually a small frequency shift (up to 30 cm^{-1}) between pairs of corresponding peaks in the two sets of spectra.

C. Theoretical results

Selected bound-state energies of $BrHI^-$ and $BrDI^-$ are given in Tables II and III (for initial $J=0$, obtained with the truncation/recoupling code) along with the corresponding assignments based on inspection of expectation values of the Jacobi coordinates and visual analysis of the wave functions. The RVIB3 code produced nearly identical results. Inspection of these wave functions revealed extensive mode mixing between the bending and the H-atom stretch modes due to Fermi resonance. For example, there is a strong mixing between the $(v_1\,v_2\,v_3)=(0\,0\,1)$ and $(0\,2\,0)$ zero-order states. To demonstrate this, a simple deperturbation procedure was performed, where the sum and difference of these two eigenstates were determined. Contour plots of the resulting wave functions, along with the original eigenstates, are shown in Fig. 3. The two top plots in Fig. 3 show the two-dimensional cuts of the wave functions of the 983 and 1228 cm^{-1} eigenstates, whereas the two bottom plots present the sum (on the left) and the difference (on the right) of these two wave functions. After the deperturbation process, the two unassignable eigenstates become the (0 2 0) state (for the sum) and the (0 0 1) state (for the difference). The bend overtone (as opposed to the fundamental) is assigned based on the presence of two nodes along the angular coordinate, only half of which is shown in the figure. As a result of these observations, a special assignment representation has been used to indicate the Fermi resonances formed by two pure states.

The transition energies calculated using the Jacobi coordinate truncation/recoupling procedure and infrared intensi-

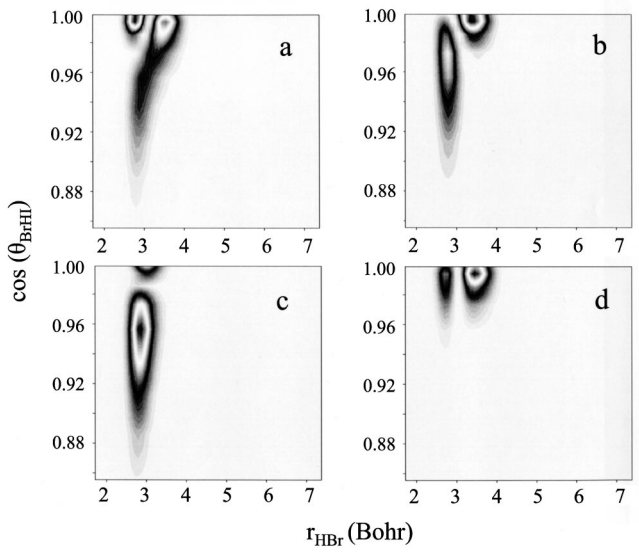

FIG. 3. Contour plots of the eigenfunctions at (a) 983.2 and (b) 1126.9 cm^{-1}, and (c) sum and (d) difference of the two, representing the pure states of the bending overtone and the H-atom stretch modes, respectively. The plots are two-dimensional slices in the plane defined by r_{HBr} and the bond angle θ_{BrHI}.

ties calculated by the RVIB3 code are listed in Tables II and III. These have been scaled relative to the highest intensity, which is assigned to unity. The relative intensities are shown against the predissociation spectra of $BrHI^-$ and $BrDI^-$ in Fig. 4. In this figure, the experimental data are plotted on a logarithmic scale for reasons discussed in Sec. IV A. The correspondence between the calculated and the experimental peak positions is strikingly clear, and the intensities of the strongest peaks are also in good agreement. There is more divergence between the theoretical and experimental intensities for many of the smaller features, with considerably more dynamic range in the calculated values.

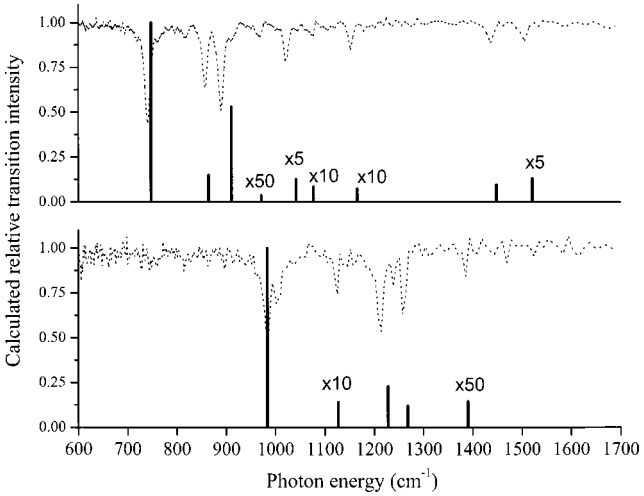

FIG. 4. Comparison of the predissociation spectra (dotted traces) with the calculated frequencies and intensities based on the dipole moment matrix elements. The lower portion shows $BrHI^-$; $BrDI^-$ is shown above it. The experimental data are normalized to the background and shown on a logarithmic scale. Calculated intensities are normalized to the largest intensity and plotted on a linear scale for comparison.

To estimate the effect of argon on the vibrations of $BrHI^-$, we optimized the $BrHI^- \cdot Ar$ complex using the CCSD(T) method with the AVTZ basis and ECP for Br, I, and Ar atoms. Three stationary structures were located with binding energy ranging from 275 to 377 cm^{-1}. The lowest energy structure has a *T*-shaped geometry with the Ar atom closer to I than to the Br atom. A full normal-mode analysis at the three stationary points revealed shifts in the $BrHI^-$ modes of at most 5 and 13 cm^{-1} for the bending and H-atom stretch harmonic frequencies, respectively. Although this is slightly smaller than some of the shifts observed in the experiment, it is clear from the full-dimensional simulations that harmonic frequencies are not sufficient to describe quantitatively the vibrational energies of these anions. Regardless, interpretation of the experimental data must not assume unreasonably large argon shifts.

V. ANALYSIS AND DISCUSSION

A. VPD spectra

The close correspondence between the matrix work of Ellison and Ault[10] and peaks *A* and *C* in our VPD spectra would suggest the same assignment for our spectra as were assigned to the matrix, namely, that peaks *A* and *C* are the (0 0 1) and $(0\ n\ 0)$ transitions, with $n=1$ or 2. On the other hand, Kaledin *et al.*[17] calculated the (0 0 1) and (0 2 0) transitions in $BrHI^-$ to lie slightly to the blue of the gas phase peaks *C* and *A*, respectively, at 1266 and 1026 cm^{-1}. This result suggests that the matrix assignment needs to be reversed. Neither assignment, however, explains why the two transitions are of comparable intensity; as shown earlier, the harmonic calculations predict the (0 0 1) transition to be considerably more intense than the bending fundamental, let alone the overtone. In addition, assigning either peak *A* or *C* to the (0 2 0) transition is somewhat awkward, as there is no corresponding (0 1 0) transition at approximately half the frequency in the gas phase infrared spectrum or in the matrix. Assignment of the $BrHI^-$ and $BrDI^-$ VPD spectra is therefore less straightforward than might be expected for a triatomic molecule.

The ambiguity regarding the assignment of the major peaks is removed by the calculations presented here, in which we determine accurate ro-vibrational eigenstates and eigenfunctions on a high-level, three-dimensional potential-energy surface. These new calculations show a significant degree of mode mixing between the bending and the H-atom stretch modes. Consequently, peaks *A* and *C* are best described as transitions to $(0\ 2\ 0 \pm 0\ 0\ 1)$ states, both of which have significant zero-order bend and H-atom stretch character. The striking agreement between the experiment and simulated peak positions, as shown in Tables II and III, is compelling evidence for the assignments provided in those tables and an indication that the potential energy surface used here is satisfactory to describe the vibrational modes of the $BrHI^-$ and $BrDI^-$ anions. The strong mode mixing also explains the comparable intensities of peaks *A* and *C* because each eigenstate has a significant (0 0 1) admixture.

The calculations support our conjecture in Sec. IV A that peaks *B* and *D* in the $BrHI^- \cdot Ar$ spectrum and peaks *B*, *D*, *E*,

F, and *G* are combination bands based on peaks *A* and *C* involving the low-frequency v_1 mode. The calculated frequencies and assignments based on the wave-function analysis are given in Tables II and III. The calculations also suggest assignments for the two highest energy peaks *H* and *I* in the $BrDI^- \cdot Ar$ spectrum to the (0 4 0±0 0 2) transitions. The small peaks *a* and *c* in the $BrHI^- \cdot Ar$ spectrum are also identified in Table II as the addition of some mode involving the argon atom. The spacings of peaks *a* and *c* from peaks *A* and *C*, respectively, is approximately the same as in $BrHBr^- \cdot Ar$,[8] where similar argon modes were observed.

Overall, the agreement between the experimental and calculated peak positions is excellent, as can be seen in Tables II and III and in Fig. 4. However, the intensities do not agree nearly as well. Many of the smaller peaks are considerably more intense in the experimental VPD spectra than in the calculations, particularly the combination bands involving excitation of the v_1 mode. This discrepancy may reflect saturation effects in the experiment; the FEL beam does not fully overlap the trapped ions, so even if all the ions in the laser field are excited, one would not observe a 100% depletion. This effect reduces the relative intensity of the strongest transitions in the experiment, making the weaker peaks look more intense than they actually are. It is also possible that anharmonic effects involving the v_1 mode are underestimated in the calculations. However, the v_1 combination bands to the blue of peaks *A* and *C* are essentially absent from the matrix absorption spectra, lending support to the intensity discrepancies originating in the VPD spectra rather than in the calculations.

Finally, the full ro-vibrational calculations find the (0 1 0) transition strength to be comparable to that of the (0 0 1) transition, in contrast to the harmonic results. It thus appears that the harmonic approximation breaks down badly even in describing the bend fundamental of $BrHI^-$. The calculated positions for the (0 1 0) peaks of $BrHI^-$ and $BrDI^-$ are 597.2 and 426.8 cm^{-1}, respectively. This result has interesting implications for the matrix IR spectra because the 666 cm^{-1} peak for $BrHI^-$ and 470 cm^{-1} peak for $BrDI^-$, which were originally assigned to the type II structure, could actually be the (0 1 0) peaks, both blueshifted by less than 70 cm^{-1} from the calculated values. This assignment would imply that only one form of the anion exists in the matrix. The observation of (0 1 0) transitions in the gas phase experiments near the calculated values would confirm this new interpretation. Unfortunately, the calculated (0 1 0) frequency for $BrDI^-$ is well below the lowest frequency available to the gas phase experiment in its current configuration, 590 cm^{-1}, whereas that for $BrHI^-$ is very close to this lower limit and may also be out of range.

B. Multiphoton spectra

There are clearly more peaks in the multiphoton spectra than in the VPD spectra, and the additional peaks appear to cluster near the frequencies at which peaks *A* and *C* are observed in the VPD spectra. In the frequency range probed by our experiments, four to ten photons are required to reach the dissociation limit of $BrHI^-$. Moreover, a triatomic anion is less favorable for resonant IRMPD than the larger systems we have studied with this method[22,23] owing to the lower density of states at comparable levels of vibrational excitation. Under these circumstances, it is not totally unexpected that the VPD and the IRMPD spectra are not identical, presenting us with the challenge of assigning the extra peaks in the IRMPD spectra.

The additional peaks could be vibrational hot bands, but these should be largely eliminated in the spectra because the ions are cooled by collisions with cold He atoms in the ion trap prior to the interaction with the laser pulse. Alternatively, these bands could result from multiphoton transitions in which two (or more) photons are resonant with a vibrational transition in the anion. The photon energies at which these transitions would be excited will be shifted from the single-photon transitions owing to anharmonicities in the anion. While such transitions would normally be very weak, we point out that the peak intensities of the FEL are quite high (10–100 MW/cm^2). In addition, resonant excitation to a higher-lying vibrational level, i.e., an overtone versus a fundamental, should result in more facile subsequent multiphoton absorption and dissociation.

In order to explore this possibility further, the energies of several vibrational levels of $BrHI^-$ and $BrDI^-$ lying at about twice the frequency of those seen in the VPD spectra were calculated and tabulated in Tables IV and V; assuming that these are accessible by two-photon transitions, the photon energy at which each level would be excited is given in square brackets. The calculated peak positions are listed alongside the experimental peak positions. In doing so, one finds a remarkably good agreement with both the one- and the two-photon transitions. For example, a comparison of the five peaks in the lowest energy cluster for $BrHI^-$ (collectively labeled as A' in Table IV) shows that no pair of calculated and experimental frequencies differs by more than 5 cm^{-1}, supporting the proposed assignments. The correspondence between experiment and theory for some of the highest energy transitions is tenuous because the experimental peaks are barely above the noise level.

The assignments given in Tables IV and V have the seemingly undesirable feature that the most intense peak in a particular cluster is often a two-photon rather than a one-photon transition. For example, in $BrHI^-$, the most intense peak at 971 cm^{-1} is assigned as the two-photon transition to the (0 4 0+0 0 2) level, whereas the less-intense neighboring peak at 988 cm^{-1} is assigned as the one-photon transition to the (0 2 0+0 0 1) level. However, as discussed earlier, the intensities in the multiphoton spectra do not necessarily represent the transition strengths, because subsequent absorption from higher-lying levels is expected to be more facile. Similarly, one might expect that the one-photon transition to the (0 4 0+0 0 2) level in $BrDI^-$ (peak H' at 1442 cm^{-1}, Fig. 2) would be more intense than the two-photon transition to the same level (peak A' at 719 cm^{-1}). Here, however, there is the additional compensating factor that the FEL intensity is about a factor of 3 lower at peak H' compared to peak A'.

Finally, as can be seen from the tables, the peaks in the VPD and IRMPD spectra assigned to the same transitions

occur at slightly different energies. These shifts are largest at lower photon energies and appear to be more significant for $BrDI^-$ than for $BrHI^-$, as can be seen by inspection of the two sets of spectra in Figs. 1 and 2. In $BrHI^-$, the shifts due to argon are at most 13 cm^{-1}, much smaller than in $BrDI^-$, where several shifts larger than 20 cm^{-1} are present. Some of the larger shifts in $BrDI^-$ may reflect ambiguities in the assignment of the IRMPD spectra. For example, the (1 2 0+1 0 1) peak (*B* in the VPD spectrum, *B′* in the IRMPD spectrum), which shows no discernible shift upon addition of the argon atom in $BrHI^-$, shows a shift in $BrDI^-$ of 29 cm^{-1} to the red. In the case of the $BrDI^-$ multiphoton spectrum, the (1 2 0+1 0 1) transition could also have been assigned to the peak at 848 cm^{-1}, for a shift of only 9 cm^{-1} (this time to the blue). However, assigning the very weak peak at 848 cm^{-1} to an allowed one-photon transition seems less desirable than the assignment given in Table V. The question arises as to whether these shifts are from Ar complexation, the multiphoton nature of the IRMPD process, or some combination of the two. In fact, the shifts in the $BrHI^- \cdot Ar$ VPD spectrum relative to the bare-ion IRMPD spectrum are within the range expected for the Ar complexation, as predicted by the harmonic calculations in Sec. IV C. The origin of the larger shifts in $BrDI^-$ are less clear at this time and their interpretation may require a more sophisticated theoretical treatment of the vibrational energy levels in $BrHI^- \cdot Ar$.

VI. SUMMARY

The gas phase vibrational predissociation of $BrHI^- \cdot Ar$ and $BrHI^- \cdot Ar$ and multiphoton dissociation spectra of $BrHI^-$ and $BrDI^-$ have been measured using a tunable infrared free-electron laser. In addition, high-level calculations of the anion potential energy surface and the vibrational eigenstates and eigenfunctions supported by this surface have been carried out. Comparison of the experimental and theoretical results leads to a detailed assignment of all the spectral features. Multiphoton dissociation spectra revealed some additional structure assigned to transitions to higher-energy states via two-photon transitions.

The gas phase frequencies observed here are close to those seen in earlier matrix-isolation experiments and attributed to the type I form of the anion. However, our assignment differs from the original assignment of the matrix spectra. In particular, the calculated vibrational energy levels show a remarkable extent of mode mixing between the H-atom stretch and the bend modes, which manifests itself in numerous Fermi resonance states, leading to a more complex spectrum than would be expected otherwise. These mixed states help explain the difficulties in modeling the system under the harmonic approximation, both because of the perturbation of states and because of the extreme mechanical anharmonicity, that allows those perturbations. The work presented here also suggests that the matrix features attributed to the symmetric (type II) anion may arise from the bend fundamental and/or the associated combination band with the heavy atom stretch rather than that from a form of the ion different from that seen in the gas phase.

ACKNOWLEDGMENTS

This work is supported by the Specialized Research Center 546 and the Ph.D. Graduate Study Program 788 of the German Research Foundation DFG. The authors gratefully acknowledge the support of the *Stichting voor Fundamenteel Onderzoek der Materie* (FOM) in providing the required beam time on FELIX and highly appreciate the skillful assistance of the FELIX staff. C.K., C.C.U., and K.R.A. gratefully acknowledge the helpful discussions with and technical expertise from Professor Ludger Wöste, Professor Gerard Meijer, and Dr. Gert von Helden. D.M.N. thanks the Air Force Office of Scientific Research for the support under Grant No. F49620-03-1-0085. A.O. thanks the Swiss National Science Foundation for funding. J.M.B. thanks the National Science Foundation (Grant Nos. CHE-0131482 and ITR CHE-0219331) for funding.

[1] G. C. Pimentel, J. Chem. Phys. **19**, 446 (1951).
[2] G. A. Landrum, N. Goldberg, and R. Hoffman, J. Chem. Soc. Dalton Trans. **1997**, 3605.
[3] G. Caldwell and P. Kebarle, Can. J. Chem. **63**, 1399 (1985).
[4] K. Kawaguchi, J. Chem. Phys. **88**, 4186 (1988).
[5] D. M. Neumark, Acc. Chem. Res. **26**, 33 (1993).
[6] D. M. Neumark, PhysChemComm **5**, 76 (2002).
[7] B. S. Ault, Acc. Chem. Res. **15**, 103 (1982).
[8] N. L. Pivonka, C. Kaposta, M. Brummer, G. von Helden, G. Meijer, L. Wöste, D. M. Neumark, and K. R. Asmis, J. Chem. Phys. **118**, 5275 (2003).
[9] K. Kawaguchi and E. Hirota, J. Chem. Phys. **87**, 6838 (1987).
[10] C. M. Ellison and B. S. Ault, J. Phys. Chem. **83**, 832 (1979).
[11] B. S. Ault, J. Phys. Chem. **83**, 837 (1979).
[12] S. E. Bradforth, A. Weaver, D. W. Arnold, R. B. Metz, and D. M. Neumark, J. Chem. Phys. **92**, 7205 (1990).
[13] Z. Liu, H. Gomez, and D. M. Neumark, Chem. Phys. Lett. **332**, 65 (2000).
[14] R. B. Metz and D. M. Neumark, J. Chem. Phys. **97**, 962 (1992).
[15] S. G. Lias, J. E. Bartmess, J. F. Liebman, J. L. Holmes, R. D. Levin, and W. G. Mallard, J. Phys. Chem. Ref. Data **17**, 1 (1988).
[16] M. Broïda and A. Persky, Chem. Phys. **133**, 405 (1989).
[17] A. Kaledin, S. Skokov, J. M. Bowman, and K. Morokuma, J. Chem. Phys. **113**, 9479 (2000).
[18] K. P. Huber and G. Herzberg, *Molecular Spectra and Molecular Structure IV: Constants of Diatomic Molecules* (Van Nostrand-Reinhold, New York, 1977).
[19] G. von Helden, D. van Heijnsbergen, and G. Meijer, J. Phys. Chem. A **107**, 1671 (2003).
[20] G. von Helden, I. Holleman, G. M. H. Knippels, A. F. G. van der Meer, and G. Meijer, Phys. Rev. Lett. **79**, 5234 (1997).
[21] H. Piest, G. von Helden, and G. Meijer, J. Chem. Phys. **110**, 2010 (1999).
[22] N. L. Pivonka, C. Kaposta, G. von Helden, G. Meijer, L. Wöste, D. M. Neumark, and K. R. Asmis, J. Chem. Phys. **117**, 6493 (2002).
[23] K. R. Asmis, N. L. Pivonka, G. Santambrogio, M. Brummer, C. Kaposta, D. M. Neumark, and L. Wöste, Science **299**, 1375 (2003).
[24] M. Okumura, L. I. Yeh, and Y. T. Lee, J. Chem. Phys. **83**, 3705 (1985).
[25] E. J. Bieske, S. A. Nizkorodov, O. Dopfer, J. P. Maier, R. J. Strickland, B. J. Cotterell, and B. J. Howard, Chem. Phys. Lett. **250**, 266 (1996).
[26] P. Ayotte, C. G. Bailey, G. H. Weddle, and M. A. Johnson, J. Phys. Chem. A **102**, 3067 (1998).
[27] K. R. Asmis, M. Brummer, C. Kaposta, G. Santambrogio, G. von Helden, G. Meijer, K. Rademann, and L. Wöste, Phys. Chem. Chem. Phys. **4**, 1101 (2002).
[28] M. Dolg, Ph.D. thesis, Universität Stuttgart, 1989.
[29] MOLPRO is a package of ab initio programs written by H.-J. Werner and P. J. Knowles, with contributions from R. D. Amos, A. Berning, D. L. Coo-

per, M. J. O. Deegan, A. J. Dobbyn, F. Eckert, C. Hampel, G. Hetzer, T. Leninger, R. Lindh, A. W. Lloyd, W. Meyer, M. E. Mura, A. Nicklaß, P. Palmieri, K. Peterson, R. Pitzer, P. Pulay, G. Rauhut, M. Schütz, H. Stoll, A. J. Stone, and T. Thorsteinsson.

[30] W. Müller, J. Flesch, and W. Meyer, J. Chem. Phys. **80**, 3297 (1984).

[31] S. Carter, N. C. Handy, R. Puzzarini, R. Tarroni, and P. Palmieri, Mol. Phys. **98**, 1713 (2000).

[32] S. Carter, N. C. Senekowitsch, N. C. Handy, and P. Rosmus, Mol. Phys. **65**, 143 (1988).

[33] T. Taketsugu, K. Ishii, and S. Carter, Chem. Phys. Lett. **380**, 213 (2003).